Electronic Supplementary Information for the paper

Electronic Structure-based rate rules for Ḣ ipso addition-elimination reactions on mono-aromatic hydrocarbons with single and double OH/CH_3/OCH_3/CHO/C_2H_5 substituents: a systematic theoretical investigation

*Luna Pratali Maffei, Tiziano Faravelli, Carlo Cavallotti, Matteo Pelucchi**

CRECK Modelling Lab, Department of Chemistry, Materials and Chemical Engineering "G. Natta", Politecnico di Milano, P.zza Leonardo da Vinci 32, 20133 Milano, Italy

*Corresponding author: Dr. Matteo Pelucchi, Dipartimento di Chimica, Materiali e Ing. Chimica "G. Natta", Politecnico di Milano, P.zza Leonardo da Vinci 32, 20133 Milano, Italy.

e-mail: matteo.pelucchi@polimi.it

Table of contents

1. **Potential energy surfaces**
2. **Rate constants: fits with modified Arrhenius expression for Ḣ-addition channel**
3. **Global backward rate constants plots**
4. **Comparison with literature data**
5. **Impact of the exit complex in the ȮH elimination channel**
6. **Energetics comparison among different reaction channels**
7. **Rate Rules derivation**
8. **Stabilization of the intermediate well**
9. **Pre-exponential factors analysis**

Attached files: mess input files, Arrhenius fits of the elementary reaction channels of each PES.

1. Potential energy surfaces

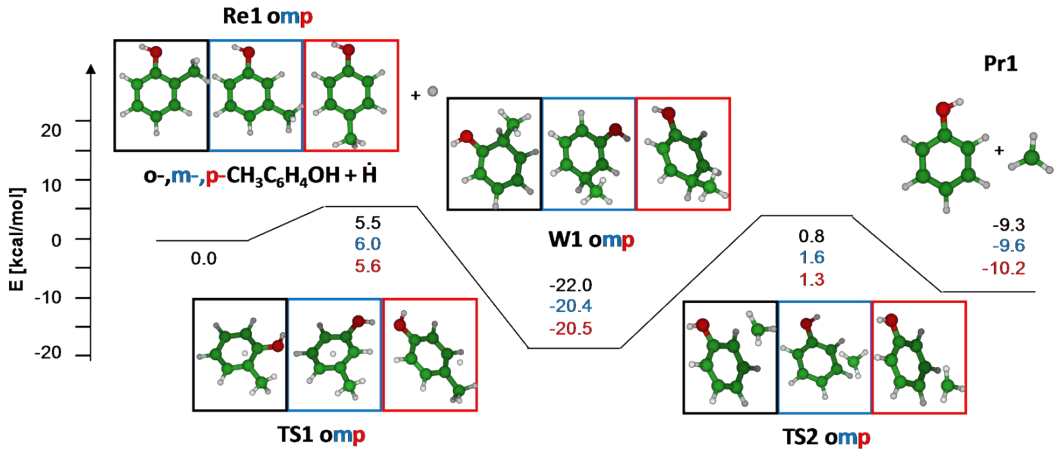

Figure S1: PESs of the o-,m-,p-$CH_3C_6H_4OH$+Ḣ=C_6H_5OH+$\dot{C}H_3$ reaction. Energies in kcal/mol are computed with respect to the reactants o-,m-,p-$CH_3C_6H_4OH$+Ḣ and are inclusive of zero point energies. The names of the stationary points correspond to those of the attached MESS input files.

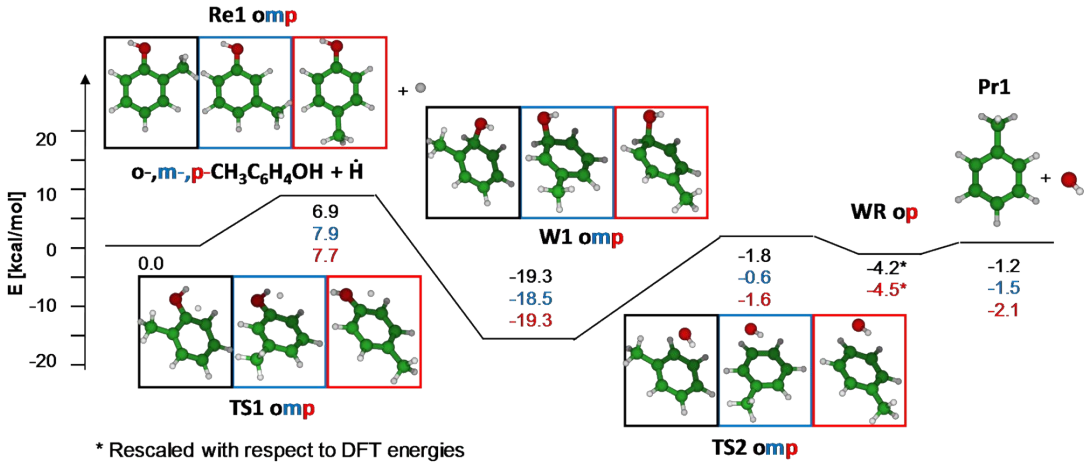

Figure S2: PESs of the o-,m-,p-$CH_3C_6H_4OH$+Ḣ=C_7H_8+$\dot{O}H$ reaction. Energies in kcal/mol are computed with respect to the reactants o-,m-,p-$CH_3C_6H_4OH$+Ḣ and are inclusive of zero point energies. The names of the stationary points correspond to those of the attached MESS input files. We were unable to find an entrance WR for ȮH addition to toluene in the meta position.

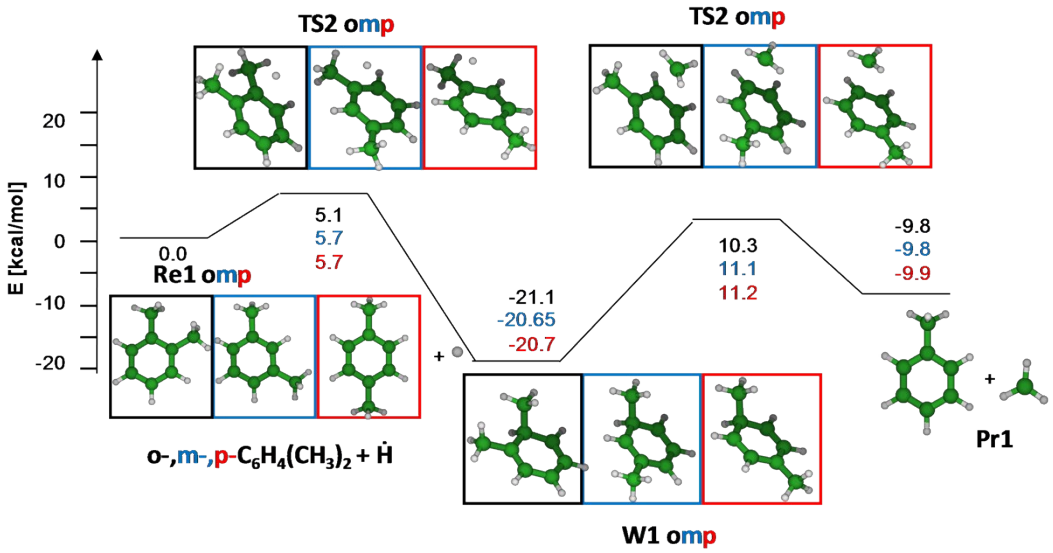

Figure S3: PESs of the o-,m-,p-$CH_3C_6H_4CH_3$+Ḣ=C_7H_8+$\dot{C}H_3$ reaction. Energies in kcal/mol are computed with respect to the reactants o-,m-,p-$CH_3C_6H_4CH_3$+Ḣ and are inclusive of zero point energies. The names of the stationary points correspond to those of the attached MESS input files.

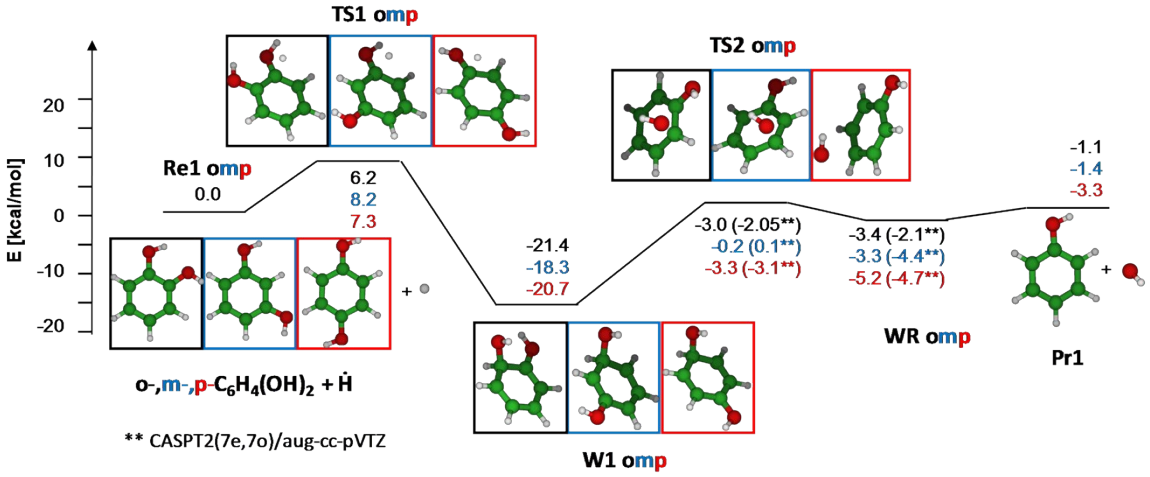

Figure S4: PESs of the o-,m-,p-OHC_6H_4OH+Ḣ=C_6H_5OH+$\dot{O}H$ reaction. Energies in kcal/mol are computed with respect to the reactants o-,m-,p-OHC_6H_4OH+Ḣ and are inclusive of zero point energies. The names of the stationary points correspond to those of the attached MESS input files.

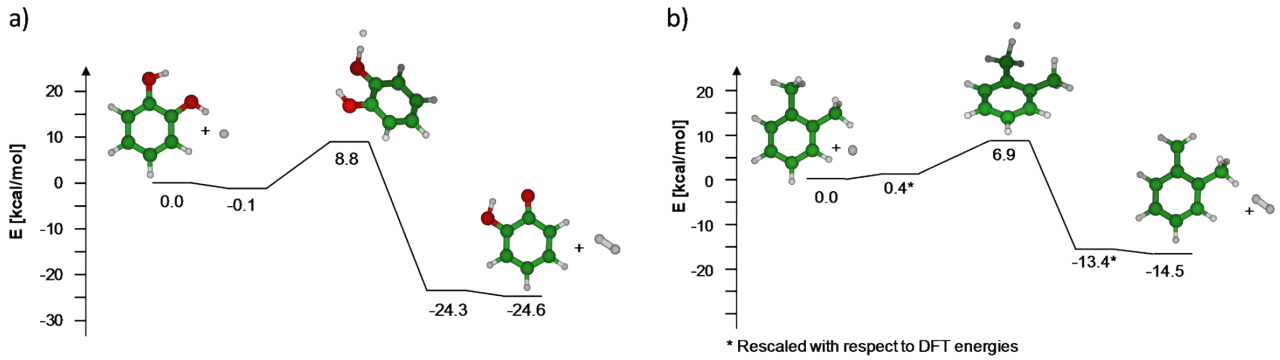

Figure S5: PES of the H-atom abstraction on the hydroxy group of catechol a) and on the methyl group of o-xylene b), computed at the CCSD(T)/CBS//m06-2X/6-311+g(d,p) level consistently with our recent work on H-atom abstraction reactions on several singly-substituted MAHs.[1] *Energies are computed with respect to the reactants and are inclusive of zero point energies.*

2. Rate constants: fits with modified Arrhenius expression for Ḣ-addition channel

Table S1: 3-parameter Arrhenius fits in the 300-2000 K range of the calculated global rate constants for Ḣ-addition to R'C_6H_4R for all the reactions computed in this work. The level of theory of the calculations is reported in Table 3 of the main text. Light shaded areas represent the rate constants used for validation, consistently with the tables in the main text. $k = k_0 T^{1.71} exp(-E_A/RT)$, *units are cm, mol, s, cal.* $R^2 > 0.998$ *for every reaction. The rate constants are on a single-site basis (i.e. when R'=R,* k_0 *was divided by 2).*

	$k_0\ [s^{-1}]$	α	$E_A\left[\frac{cal}{mol}\right]$	$\frac{k_{0,R}^{R'}}{k_{0,H}^{R'}}$	Control population
$C_6H_5OH + Ḣ \rightarrow C_6H_6 + ȮH$	5.37E+07	1.71	5899.84		
o-$OHC_6H_4CH_3 + Ḣ \rightarrow C_6H_5CH_3 + ȮH$	5.27E+07	1.71	4776.98	0.98	
m-$OHC_6H_4CH_3 + Ḣ \rightarrow C_6H_5CH_3 + ȮH$	4.89E+07	1.71	5702.84	0.91	
p-$OHC_6H_4CH_3 + Ḣ \rightarrow C_6H_5CH_3 + ȮH$	5.42E+07	1.71	5537.09	1.01	
o-$OHC_6H_4OH + Ḣ \rightarrow C_6H_5OH + ȮH$	5.31E+07	1.71	4753.79	0.99	
m-$OHC_6H_4OH + Ḣ \rightarrow C_6H_5OH + ȮH$	4.81E+07	1.71	5931.29	0.90	
p-$OHC_6H_4OH + Ḣ \rightarrow C_6H_5OH + ȮH$	4.32E+07	1.71	5146.11	0.80	
o-$OHC_6H_4OCH_3 + Ḣ \rightarrow C_6H_5OCH_3 + ȮH$	4.94E+07	1.71	4777.15	0.92	
m-$OHC_6H_4OCH_3 + Ḣ \rightarrow C_6H_5OCH_3 + ȮH$	4.92E+07	1.71	5901.31	0.92	
p-$OHC_6H_4OCH_3 + Ḣ \rightarrow C_6H_5OCH_3 + ȮH$	4.60E+07	1.71	4881.47	0.86	
o-$OHC_6H_4CHO + Ḣ \rightarrow C_6H_5CHO + ȮH$	4.78E+07	1.71	5622.90	0.89	
m-$OHC_6H_4CHO + Ḣ \rightarrow C_6H_5CHO + ȮH$	5.59E+07	1.71	6363.72	1.04	
p-$OHC_6H_4CHO + Ḣ \rightarrow C_6H_5CHO + ȮH$	4.95E+07	1.71	5886.72	0.92	
o-$OHC_6H_4C_2H_5 + Ḣ \rightarrow C_6H_5C_2H_5 + ȮH$	4.44E+07	1.71	4980.23	0.83	
m-$OHC_6H_4C_2H_5 + Ḣ \rightarrow C_6H_5C_2H_5 + ȮH$	5.47E+07	1.71	5842.72	1.02	
p-$OHC_6H_4C_2H_5 + Ḣ \rightarrow C_6H_5C_2H_5 + ȮH$	5.54E+07	1.71	5589.00	1.03	
$C_6H_5CH_3 + Ḣ \rightarrow C_6H_6 + ĊH_3$	5.28E+07	1.71	4387.13		
o-$CH_3C_6H_4CH_3 + Ḣ \rightarrow C_6H_5CH_3 + ĊH_3$	5.03E+07	1.71	3531.08	0.95	
m-$CH_3C_6H_4CH_3 + Ḣ \rightarrow C_6H_5CH_3 + ĊH_3$	5.54E+07	1.71	4199.20	1.05	
p-$CH_3C_6H_4CH_3 + Ḣ \rightarrow C_6H_5CH_3 + ĊH_3$	5.37E+07	1.71	4151.36	1.02	
o-$CH_3C_6H_4OH + Ḣ \rightarrow C_6H_5OH + ĊH_3$	5.08E+07	1.71	3738.60	0.96	
m-$CH_3C_6H_4OH + Ḣ \rightarrow C_6H_5OH + ĊH_3$	4.89E+07	1.71	4426.65	0.93	
p-$CH_3C_6H_4OH + Ḣ \rightarrow C_6H_5OH + ĊH_3$	4.77E+07	1.71	4022.33	0.90	
o-$CH_3C_6H_4OCH_3 + Ḣ \rightarrow C_6H_5OCH_3 + ĊH_3$	5.24E+07	1.71	3493.87	0.99	
o-$CH_3C_6H_4CHO + Ḣ \rightarrow C_6H_5CHO + ĊH_3$	5.37E+07	1.71	3668.93	1.02	
o-$CH_3C_6H_4C_2H_5 + Ḣ \rightarrow C_6H_5C_2H_5 + ĊH_3$	4.00E+07	1.71	3680.37	0.76	
$C_6H_5OCH_3 + Ḣ \rightarrow C_6H_6 + ȮCH_3$	4.86E+07	1.71	5173.05		
o-$OCH_3C_6H_4CH_3 + Ḣ \rightarrow C_6H_5CH_3 + ȮCH_3$	4.81E+07	1.71	4309.97	0.99	
o-$OCH_3C_6H_4OH + Ḣ \rightarrow C_6H_5OH + ȮCH_3$	3.01E+07	1.71	3448.12	0.62	
m-$OCH_3C_6H_4OH + Ḣ \rightarrow C_6H_5OH + ȮCH_3$	4.14E+07	1.71	5362.08	0.85	
p-$OCH_3C_6H_4OH + Ḣ \rightarrow C_6H_5OH + ȮCH_3$	4.11E+07	1.71	4415.20	0.85	
o-$OCH_3C_6H_4OCH_3 + Ḣ \rightarrow C_6H_5OCH_3 + ȮCH_3$	4.48E+07	1.71	3952.10	0.92	
o-$OCH_3C_6H_4C_2H_5 + Ḣ \rightarrow C_6H_5C_2H_5 + ȮCH_3$	3.42E+07	1.71	4172.42	0.70	
$C_6H_5CHO + Ḣ \rightarrow C_6H_6 + ĊHO$	7.50E+07	1.71	4698.78		
o-$CHOC_6H_4CH_3 + Ḣ \rightarrow C_6H_5CH_3 + ĊHO$	6.69E+07	1.71	3709.31	0.89	
o-$CHOC_6H_4OH + Ḣ \rightarrow C_6H_5OH + ĊHO$	8.45E+07	1.71	4910.90	1.13	
m-$CHOC_6H_4OH + Ḣ \rightarrow C_6H_5OH + ĊHO$	7.39E+07	1.71	4546.05	0.98	
p-$CHOC_6H_4OH + Ḣ \rightarrow C_6H_5OH + ĊHO$	7.27E+07	1.71	4660.01	0.97	
o-$CHOC_6H_4CHO + Ḣ \rightarrow C_6H_5CHO + ĊHO$	5.97E+07	1.71	3809.35	0.80	
$C_6H_5C_2H_5 + Ḣ \rightarrow C_6H_6 + Ċ_2H_5$	4.96E+07	1.71	4193.25		
o-$C_2H_5C_6H_4CH_3 + Ḣ \rightarrow C_6H_5CH_3 + Ċ_2H_5$	4.04E+07	1.71	3202.42	0.82	
o-$C_2H_5C_6H_4OH + Ḣ \rightarrow C_6H_5OH + Ċ_2H_5$	4.51E+07	1.71	3333.42	0.91	
m-$C_2H_5C_6H_4OH + Ḣ \rightarrow C_6H_5OH + Ċ_2H_5$	4.64E+07	1.71	4285.57	0.94	
p-$C_2H_5C_6H_4OH + Ḣ \rightarrow C_6H_5OH + Ċ_2H_5$	4.50E+07	1.71	3755.11	0.91	
o-$C_2H_5C_6H_4C_2H_5 + Ḣ \rightarrow C_6H_5C_2H_5 + Ċ_2H_5$	3.65E+07	1.71	3062.62	0.74	
m-$C_2H_5C_6H_4C_2H_5 + Ḣ \rightarrow C_6H_5C_2H_5 + Ċ_2H_5$	4.78E+07	1.71	4037.22	0.97	

p-$C_2H_5C_6H_4C_2H_5$ + Ḣ → $C_6H_5C_2H_5$ + Ċ$_2H_5$	4.77E+07	1.71	4033.39	0.96	

3. Global backward rate constants plots

Figure S6 shows the rate constants of the global reaction of ipso-addition of R'=ȮH, ĊH$_3$ on C$_6$H$_5$R, namely benzene (R=H, black lines), toluene (R=CH$_3$, blue lines), and phenol (R=OH, red lines). The plots group the rate constants for the ipso-addition of Ṙ' on the ortho (Figure S6a), meta (Figure S6b), and para (Figure S6c) positions with respect to R. The rate constants of Ṙ' ipso-addition on benzene are the same in each plot. In order to compare the ipso-addition rate constants on a single-site basis, the rates were divided accordingly (i.e. factor of 2 for the ortho and meta positions, factor of 6 for Ṙ' ipso-addition on benzene). It is highlighted that the impact of the lateral groups OH and CH$_3$ on the Ṙ' ipso-addition rate constants (i.e. the reverse rate constants of the Ḣ ipso-additions on o-,m-,p-R'C$_6$H$_4$R shown in Figure 6 of the main text) is less significant than for the backward rate constants of these reactions. In particular, relevant differences are observed only in the case of ipso-additions on the ortho position with respect to the R group of C$_6$H$_5$R (Figure S6a). As expected from the discussion on Ḣ ipso-additions, in these cases the energy barrier of Ṙ' ipso-addition decreases, resulting in an increase in the global rate constant. However, in absence of secondary reactivity of the formed adduct (as assumed in this work), the ipso-addition of ȮH and ĊH$_3$ on the aromatic ring is not competitive with H-abstractions by the same radicals, therefore these ipso-addition reactions have only a small impact in global combustion kinetic models.

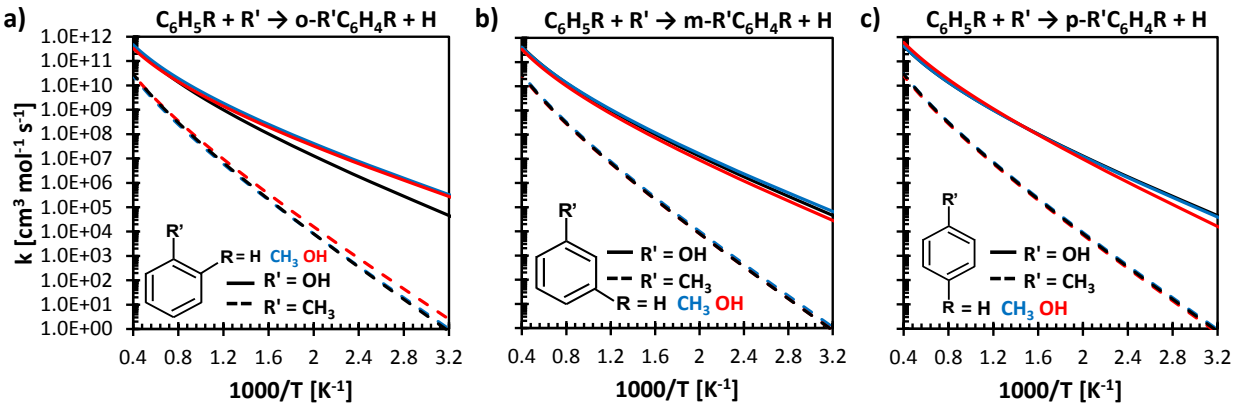

Figure S6: Plots of the rate constants of the global reactions of ipso-addition of Ṙ' on the ortho a), meta b) and para c) ring sites of C$_6$H$_5$R, where Ṙ' can be ȮH (solid lines) or ĊH$_3$ (dashed lines), and the reactant C$_6$H$_5$R can be benzene (R = H, black lines), toluene (R = CH$_3$, blue lines), or phenol (R = OH, red lines). No distinction among ortho, meta, and para ring sites is done for benzene. All the rate constants refer to ipso-addition to a single site (i.e. tot/6 for benzene, tot/2 for ortho and meta sites).

4. Comparison with literature data

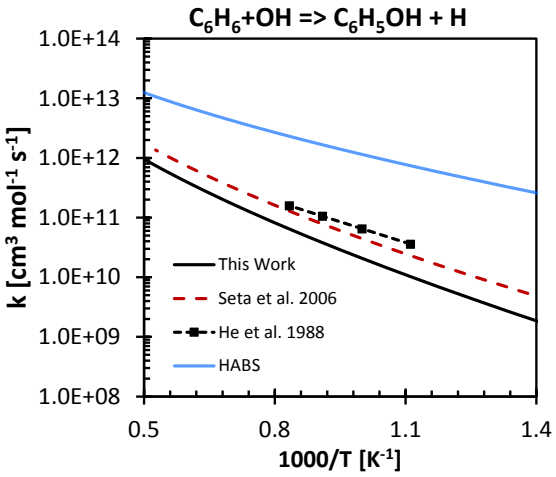

Figure S7: Comparison of the rate constant of H replacement by OH in benzene with the estimate of He et al.,[2] which was performed from the experimental measure of the rate of the backward process using the equilibrium constant, and the theoretical rate constant of Seta et al.[3] The HABS line corresponds to the rate of the H-atom abstraction by OH computed in our recent work, showing that the H-atom abstraction always prevails with respect to the H replacement channel.[1]

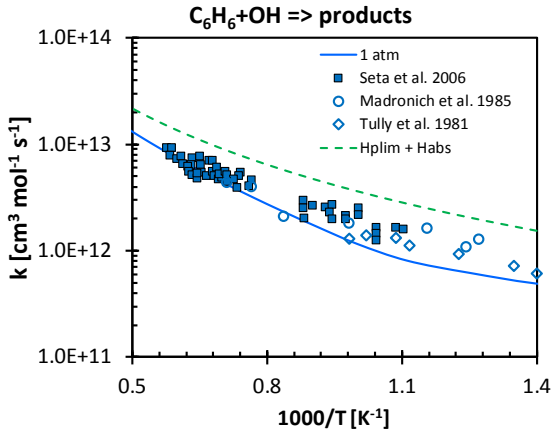

Figure S8: Rate constant of OH addition to benzene, computed as the sum of the rate constants of the adduct formation, the well-skipping rate to form phenol+H, and the H-atom abstraction reaction by OH (from [1]). The rate Hplim+Habs is the rate of the high-pressure limit channels of the same reaction. Comparison with some of the available experimental data is provided.[3–5] At low pressure, the contribution to the total rate comes entirely from the H-atom abstraction channel; at 1 atm, the substitution of H by OH plays a role only below 900 K.

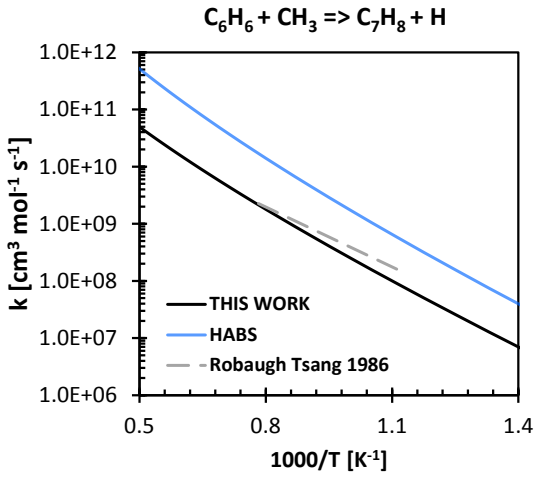

Figure S9: Comparison of the rate constant of H replacement by CH_3 in benzene with the estimate of Robaugh and Tsang[6] and with the competing H-atom abstraction by CH_3, computed in our recent work.[1] In this case, the H-atom abstraction always prevails with respect to H replacement by methyl, however to a lesser extent with respect to H replacement by OH.

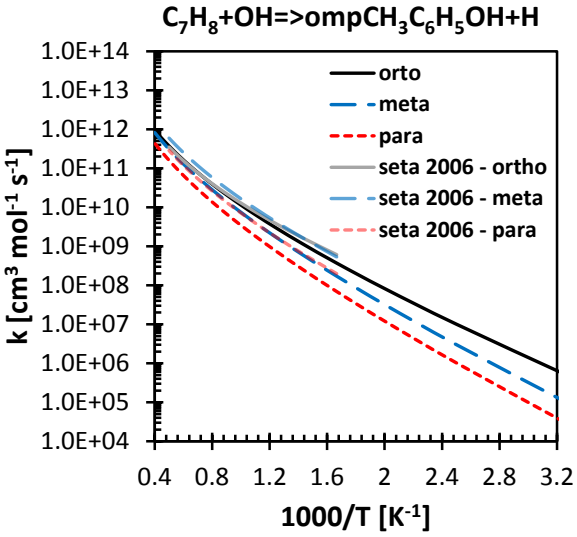

Figure S10: Rate constants of H replacement by OH in toluene to form the ortho, meta and para isomers of cresol. Comparison is provided with the estimates of Seta et al,[3] with a general agreement and a maximum discrepancy of a factor of 3 for H replacement in the meta isomer.

5. Impact of the exit complex in the ȮH elimination channel

Figure 2a depicts the PES of Ḣ ipso-addition on phenol, showing the formation of a post-reaction complex which is about 2 kcal/mol more stable than the products. According to ME calculations, the post-reaction complex collisionally stabilizes in the whole temperature range only in the case of ȮH elimination to form benzene at 1000 atm. As regards ȮH elimination to form phenol, the exit complex has a similar interaction energy (about -2 kcal/mol with respect to the products C_6H_5OH+ȮH). However, its inclusion in the ME simulations has a negligible impact (<10%) on the rate constants of both the elementary steps and the global reaction channels. In fact, due to the low energy barrier for ȮH elimination with respect to the products, the formation of the exit complex does not lead to significant tunneling.

As highlighted above, Ḣ ipso-addition on phenol was the only case in which we found that the exit van der Waals well WR of the ȮH elimination channel to form benzene impacts the backward rate constant $k_{\overleftarrow{2}}$ of the elementary step of the well dissociation to ȮH+C_6H_6. The comparison between $k_{\overrightarrow{2}}$,$k_{\overleftarrow{2}}$ when excluding or including WR in the ME simulations are shown on the left and right side of Figure S14. The comparison between the two plots shows that WR stabilizes at 1000 atm in the full range of investigated temperatures. Figure S14b shows that at 1000 atm the adduct dissociates only partially to products, as it mostly converts to WR. WR mostly dissociates back to ȮH+C_6H_6 and partially forms the adduct. As a result, WR equilibrates. However, this does not affect the global rate constants of the reaction, due to the absence of secondary reactivity of both the adduct and WR. The Arrhenius fits of the rate constants of the elementary steps are reported as txt file attached to this paper.

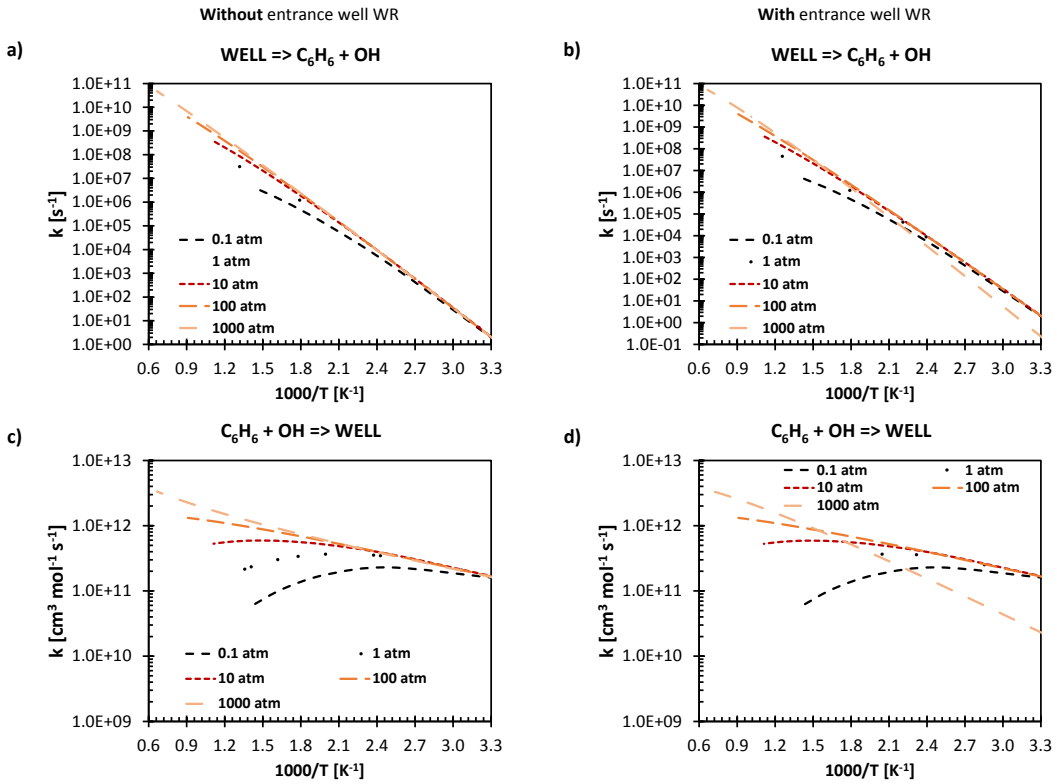

Figure S14: Rate constants $k_{\overrightarrow{2}}$,$k_{\overleftarrow{2}}$ of the elementary reaction channels of C_6H_5OH dissociation to ȮH+C_6H_6 as a function of temperature and pressure. The elementary steps of the Ḣ+C_6H_5OH addition and the well-skipping reaction channels and are not shown and are reported in a separate txt file. a) and c) show the rate constants obtained from the ME simulation for a PES that excludes the formation of the exit van der Waals complex WR, compared to b) and d) where WR is included. The PES is shown in Figure S1.

6. Energetics comparison among different reaction channels

Table S2: 0 K enthalpies [kcal/mol] of the stationary points of the PESs for the $\dot{H}+RC_6H_4R' \leftrightarrow \dot{R}'+C_6H_5R$ reactions, with R=OH,CH_3 and R'=OH,CH_3. The first row of each set corresponds to the energy of the stationary point of the PES of the singly-substituted $\dot{H}+C_6H_5R$, i.e. phenol and toluene. All the energies refer to the reactants $\dot{H}+RC_6H_4R'$ and are inclusive of zero point energies. The name of the stationary points corresponds to those of Figure S1-4 (W1 is called adduct Ȧ in the main text).

ΔE(W1)	**R=OH R'=OH**	**R=OH R'=CH_3**	**R=CH_3 R'=OH**	**R=CH_3 R'=CH_3**
R=H	-18.3	-20.3	-18.3	-20.3
ortho	-21.4	-22.0	-19.3	-21.1
meta	-18.3	-20.3	-18.5	-20.7
para	-20.7	-20.5	-19.3	-20.6

ΔE(TS1)	**R=OH R'=OH**	**R=OH R'=CH_3**	**R=CH_3 R'=OH**	**R=CH_3 R'=CH_3**
R=H	8.1	5.9	8.1	5.9
ortho	6.2	5.5	6.9	5.1
meta	8.2	6.0	7.9	5.7
para	7.3	5.6	7.7	5.7

ΔE(TS2)	**R=OH R'=OH**	**R=OH R'=CH_3**	**R=CH_3 R'=OH**	**R=CH_3 R'=CH_3**
R=H	-0.6	1.4	-0.6	1.4
ortho	-3.0	0.8	-1.8	0.5
meta	-0.2	1.6	-0.6	1.3
para	-3.3	1.3	-1.6	1.3

ΔE(Pr1)	**R=OH R'=OH**	**R=OH R'=CH_3**	**R=CH_3 R'=OH**	**R=CH_3 R'=CH_3**
R=H	-1.7	-9.8	-1.7	-9.8
ortho	-1.1	-9.3	-1.2	-9.8
meta	-1.4	-9.6	-1.5	-9.8
para	-3.3	-10.2	-2.1	-9.9

Table S3: 0 K enthalpies [kcal/mol] of the stationary points of the PESs for the $\dot{H}+RC_6H_4R' \leftrightarrow \dot{R}'+C_6H_5R$ reactions, with R=OH,CH_3 and R'=OH,CH_3, with respect to the 0 K enthalpies of the corresponding stationary points of the PES of the singly-substituted $\dot{H}+C_6H_5R'$, i.e. phenol and toluene, R=H. The energies are obtained from Table S2, subtracting in each set the first line (R=H). $\Delta E(TS2)_{R\text{-}H}$ was obtained subtracting the energy barriers of Ṙ'addition. The name of the stationary points corresponds to those of Figure 1 in the main text and Figure S1-4 (W1 is indicated as adduct Ȧ in the main text). The energies and $\Delta E(TS1)_{R\text{-}H}$ are plotted in Figure S15.

$\Delta E(W1)_{R\text{-}H}$	**R=OH R'=OH**	**R=OH R'=CH_3**	**R=CH_3 R'=OH**	**R=CH_3 R'=CH_3**
R=H	0.0	0.0	0.0	0.0
ortho	-3.1	-1.7	-1.0	-0.8
meta	0.0	0.0	-0.2	-0.3
para	-2.4	-0.2	-1.0	-0.3

$\Delta E(TS1)_{R\text{-}H}$	**R=OH R'=OH**	**R=OH R'=CH_3**	**R=CH_3 R'=OH**	**R=CH_3 R'=CH_3**
R=H	0.0	0.0	0.0	0.0
ortho	-1.9	-0.4	-1.2	-0.8
meta	0.1	0.1	-0.2	-0.2
para	-0.8	-0.3	-0.4	-0.2

$\Delta E(TS2)_{R\text{-}H}$	**R=OH R'=OH**	**R=OH R'=CH_3**	**R=CH_3 R'=OH**	**R=CH_3 R'=CH_3**
R=H	0.0	0.0	0.0	0.0
ortho	-3.0	-1.1	-1.7	-0.9
meta	0.1	0.0	-0.2	-0.1
para	-1.1	0.3	-0.6	0.0

$\Delta E(Pr1)_{R\text{-}H}$	**R=OH R'=OH**	**R=OH R'=CH_3**	**R=CH_3 R'=OH**	**R=CH_3 R'=CH_3**
R=H	0.0	0.0	0.0	0.0
ortho	0.6	0.5	0.5	0.0
meta	0.3	0.2	0.2	0.0
para	-1.6	-0.4	-0.4	-0.1

Table S4: Differences between the 0 K enthalpies computed at the CCSD(T)/CBS and ωb97-XD/6-311+g(d,p) levels of theory of the stationary points of all the 14 PESs considered in this work. The first part of the table shows the energies of the PESs of OH replacement with H (R = OH), whereas b) shows the energies of the PESs of CH_3 replacement with H (R = CH_3). R' indicates the lateral group, consistently with the notation of the rest of this work.

R = OH

R'	ADDUCT	TS1	TS2	PRODS
H	0.40	-1.86	1.09	-0.35
ortho-OH	0.96	-1.68	outlier	-0.34
meta-OH	0.22	-1.84	1.02	-0.43
para-OH	0.71	-1.67	1.69	-0.21
ortho-CH_3	0.78	-1.86	1.63	-0.18
meta-CH_3	0.33	-1.86	1.13	-0.35
para-CH_3	0.71	-1.77	1.39	-0.29
average	0.59	-1.79	1.32	-0.30
standard deviation	0.27	0.09	0.29	0.09

R = CH_3

R'	ADDUCT	TS1	TS2	PRODS
H	0.83	-2.01	-0.27	-1.00
ortho-OH	1.15	-1.92	-0.02	-0.83
meta-OH	0.74	-1.98	-0.25	-1.00
para-OH	1.07	-1.84	-0.15	-0.94
ortho-CH_3	1.09	-2.00	-0.10	-0.88
meta-CH_3	0.72	-1.98	-0.25	-0.97
para-CH_3	1.11	-1.91	-0.20	-0.94
average	0.96	-1.95	-0.18	-0.94
standard deviation	0.19	0.06	0.09	0.06

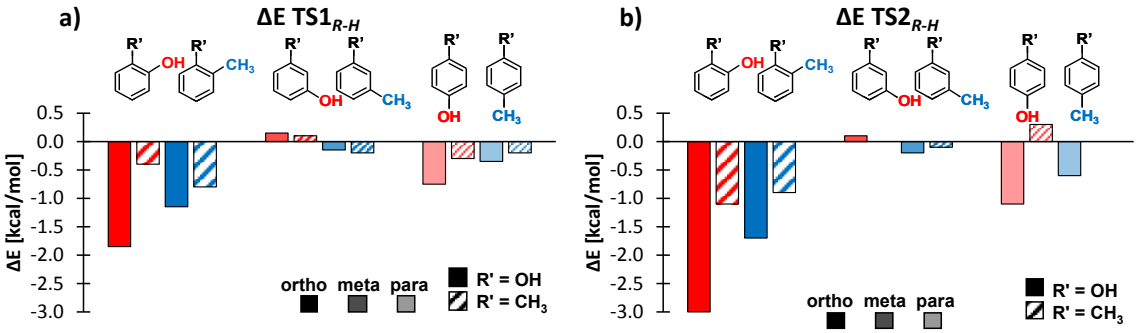

Figure S15: Effect of the R substitution (CH_3 in blue, OH in red) in the ortho, meta, and para positions with respect to the singly-substituted compound (R = H) on the relative increase of the 0 K enthalpies of the barrier of the H-addition channel ΔE(TS1) a) and of the R'-addition channel ΔE(TS2) b). The corresponding values are reported in Table S3 of the ESI.

7. Rate rules derivation

Table S5: Corrections $\Delta E_{A,R-H}^{R'}$ *of the energy barriers (kcal/mol) of the H-addition reaction to R'C_6H_4R with respect to the reference R'C_6H_5 obtained with the rate rules derived in this work. The shaded values were used as a reference for the rate rules and therefore corresponds to the original values* $\Delta E_{A,R-H}^{R'}$ *of the 3-parameter Arrhenius fits* $0.93k_{0,R=H}T^{1.71}\exp\left(-\frac{E_A}{RT}\right)$ *reported in Table 4 of the main text. The values in brackets correspond to the actual values obtained from ab-initio calculations.*

R=CH_3				
R'=OH	R'=CH_3	R'=OCH_3	R' = CHO	R' = C_2H_5
-1.2	-0.9 (-0.9)	-1.0 (-0.9)	-0.9 (-0.9)	-0.8 (-0.8)
-0.2	-0.2 (-0.3)	-0.2	-0.2	-0.2
-0.5	-0.3 (-0.3)	-0.4	-0.4	-0.3

R=OH				
R'=OH	R'=CH_3	R'=OCH_3	R' = CHO	R' = C_2H_5
-1.2	-0.9 (-0.7)	-1.1 (-1.2)	0.0	-0.9 (-0.8)
0.1	0.1 (0.0)	0.1 (0.3)	0.0 (-0.2)	0.1 (0.1)
-0.6	-0.4 (-0.3)	-0.5 (-0.6)	0.0 (-0.1)	-0.4 (-0.4)

R=OCH_3				
R'=OH	R'=CH_3	R'=OCH_3	R' = CHO	R' = C_2H_5
-1.1	-0.8 (-1.0)	-1.0 (-1.2)	-0.9	-0.8
0.0	0.0	0.0	0.0	0.0
-0.9	-0.7	-0.8	-0.7	-0.7

R=HCO				
R'=OH	R'=CH_3	R'=OCH_3	R' = CHO	R' = C_2H_5
-0.2	-0.7	-0.9	-0.8 (-0.7)	-0.7
0.3	0.3	0.3	0.3	0.3
0.0	0.0	0.0	0.0	0.0

R=C_2H_5				
R'=OH	R'=CH_3	R'=OCH_3	R' = CHO	R' = C_2H_5
-0.8	-0.6 (-0.5)	-0.7 (-0.7)	-0.6	-0.6 (-0.8)
-0.2	-0.2	-0.2	-0.2	-0.2 (-0.2)
-0.4	-0.3	-0.4	-0.3	-0.3 (-0.2)

8. Stabilization of the intermediate well

As anticipated in the main text, in combustion kinetic models the rate constants for ipso-substitution reactions are included as a "global" step $R'C_6H_4R + \dot{H} \underset{\vec{k}_{\leftarrow g}}{\overset{k_{\rightarrow g}}{\rightleftharpoons}} C_6H_5R + \dot{R}'$. However, in atmospheric chemistry the addition and beta-scission steps are generally considered separately $R'C_6H_4R + \dot{H} \underset{\vec{k}_{\leftarrow 1}}{\overset{k_{\rightarrow 1}}{\rightleftharpoons}} \dot{A} \underset{\vec{k}_{\leftarrow 2}}{\overset{k_{\rightarrow 2}}{\rightleftharpoons}} C_6H_5R + \dot{R}'$, as the adduct may show significant stabilization, and the rate constant $k_{\rightarrow 2}$ of the Ṙ'-addition channel may be 1-2 orders of magnitude higher than the global ipso substitution rate constant $k_{\rightarrow g}$.[7] The rate of ipso substitution of hydroxyl and methyl radicals (Ṙ'=ȮH, ĊH$_3$) $k_{\rightarrow g}$ is always negligible with respect to H-atom abstraction by the same radicals, whereas the rate of the elementary addition step $k_{\rightarrow 2}$ may be comparable or higher than the H-atom abstraction channel.[8]

The global rate constants $k_{\rightarrow g}$, $k_{\leftarrow g}$ were derived from the rate constants of the elementary steps according to our master equation-based lumping approach, successfully applied in our recent work on phenol pyrolysis.[9] Briefly, the procedure consists in lumping the phenomenological elementary steps describing the formation and decomposition of the adduct into a single step, through a non-linear regression of the exponential decay of the reactants concentration predicted by the integration of the full reaction network. This approach leads to a significant reduction of the pressure dependence of the rate constants of the global reactions, showing less than 10% difference in the range of investigated pressures. This is a consequence of the fact that it is the stabilization and successive reactivity of the adduct that determines the dependence of the phenomenological rate constants on pressure, so that once it is lumped the pressure dependence becomes negligible. As a result, the global rate constants may be assumed independent of pressure, as reported in the main text.

Our lumping approach assumes that the reactivity of the intermediate well is fast enough to exclude any stabilization. This is an acceptable approximation as long as its secondary reactivity is negligible. According to our ME simulations, at 1 atm the adduct is thermodynamically stable only below 800-900 K for all the reactions investigated. However, the temperature range of the stability of the adduct increases with pressure, so that it is conceivable that at high pressures and relatively low temperatures it may exhibit some secondary reactivity. Hence, we believe that our assumption is indeed valid at the conditions typical of combustion processes.

9. Pre-exponential factors analysis

In the main text, we briefly highlighted that $k_{0,R}^{R'}$ generally decrease with respect to the mono-substituted counterparts $k_{0,H}^{R'}$: $k_{0,R}^{R'}$=(0.93±0.11)$k_{0,H}^{R'}$. In this section, we discuss the factors that cause this variation in the pre-exponential factors. Consistent variations in the pre-exponential factors may be caused by tunnelling corrections, variational effects, hindered rotations, or vibrational partition functions. In this case, the imaginary frequencies of the translational motion of the adding Ḣ are very similar, resulting in maximum differences in tunnelling effects of about 30% at 300 K within each class, decreasing below 10% already at 500 K. Since this kind of variability is comparable to the errors of literature correlations which relate tunnelling factors and activation energies,[10,11] we did not develop specific corrections for tunnelling, reasonably assuming the reference reaction of each class R'C_6H_5+Ḣ to be representative of the trend for the whole class. Similarly to the findings of Miller and Klippenstein and Sabbe et al. for radical additions to unsaturated hydrocarbons,[10,12–14] tunnelling corrections are below 10% above 1000 K, however they reach factors of 1.5 around 500 K, increasing up to 2-3.5 at 300 K. Concerning variational effects, the treatment with internal coordinates results in a decrease in the rate constant within a factor of 1.2 for all $k_{\vec{1}}$, with small variations within each class R'. Regarding hindered rotations, no significant change in the rotational barriers of the reactants and the transition state is expected. In fact, hydrogen is not bulky and therefore should not result in too high hindrance of the substituents, as also noted in previous works.[10,11,15,16] This trend was generally confirmed, though higher rotational barriers and higher corresponding vibrational frequencies for internal rotations were found when R and R' substituents are in the ortho position, due to the stronger interactions between substituents. This generally explains the decrease of $k_{0,R}^{R'}$ with respect to $k_{0,H}^{R'}$. Furthermore, it seems that the bulkier the side group R, the lower the pre-exponential factor, due to the steric demand of the substituent, which contributes to the decrease in entropy of the TS with respect to the reactants. This was also noted in previous works on carbon-centered radical additions on unsaturated hydrocarbons.[11,17]

References

1 L. Pratali Maffei, M. Pelucchi, R. D. Büttgen, K. A. Heufer, T. Faravelli and C. Cavallotti, *in preparation.*

2 Y. Z. He, W. G. Mallard and W. Tsang, *J. Phys. Chem.*, 1988, **92**, 2196–2201.

3 T. Seta, M. Nakajima and A. Miyoshi, *J. Phys. Chem. A*, 2006, **110**, 5081–5090.

4 S. Madronich and W. Felder, *J. Phys. Chem.*, 1985, **89**, 3556–3561.

5 F. P. Tully, A. R. Ravlshankara, R. L. Thompson, J. M. Nicovlch, R. C. Shah, N. M. Kreutter and P. H. Wine, *J. Phys. Chem.*, 1981, **85**, 2262–2269.

6 D. Robaugh and W. Tsang, *J. Phys. Chem.*, 1986, **90**, 4159–4163.

7 G. Ghigo and G. Tonachini, *J. Am. Chem. Soc.*, 1998, **120**, 6753–6757.

8 I. V Tokmakov and M. C. Lin, *J Phys Chem A*, 2002, **106**, 11309–11326.

9 L. Pratali Maffei, M. Pelucchi, T. Faravelli and C. Cavallotti, *React. Chem. Eng.*, 2020, **5**, 452–472.

10 M. K. Sabbe, M. F. Reyniers, M. Waroquier and G. B. Marin, *ChemPhysChem*, 2010, **11**, 195–210.

11 M. K. Sabbe, M. F. Reyniers, V. Van Speybroeck, M. Waroquier and G. B. Marin, *ChemPhysChem*, 2008, **9**, 124–140.

12 M. K. Sabbe, ron G. Vandeputte, M.-F. Reyniers, V. Van Speybroeck, M. Waroquier and G. B. Marin, *J. Phys. Chem. A*, 2007, **111**, 8416–8428.

13 J. A. Miller and S. J. Klippenstein, *Phys. Chem. Chem. Phys.*, 2004, **6**, 1192–1202.

14 S. J. Klippenstein and J. A. Miller, *J. Phys. Chem. A*, 2005, **109**, 4285–4295.

15 T. N. Truong, W. T. Duncan and M. Tirtowidjojo, *Phys. Chem. Chem. Phys*, 1999, **1**, 1061–1065.

16 A. Ratkiewicz and T. N. Truong, *J. Phys. Chem. A*, 2012, **116**, 6643–6654.

17 H. Fischer and L. Radom, *Angew. Chemie Int. Ed.*, 2001, **40**, 1340–1371.